

## Thermogelling Aqueous Fluids Containing Low Concentrations of Pluronic F127 and Laponite Nanoparticles

Kunshan Sun and Srinivasa R. Raghavan\*

Department of Chemical & Biomolecular Engineering, University of Maryland, College Park, Maryland 20742-2111

Received December 29, 2009. Revised Manuscript Received April 6, 2010

The triblock copolymer Pluronic F127 (PF127) is frequently used in colloidal and pharmaceutical formulations. Concentrated aqueous solutions of PF127 (>15 wt %) are known to undergo *thermogelling* (i.e., a sol-to-gel transition upon heating), which is attributed to the formation of a volume-filling cubic array of micelles. Here, we report that thermogelling can occur at much lower PF127 concentrations (1.2 to 8 wt %) if nanoparticles of laponite (25-nm-diameter disks) are also present in the formulation. Thermogelling in laponite/PF127 mixtures requires each component to be present above a minimum level. The gels have moduli around 100 Pa, and they can be reversibly liquefied to sols upon cooling. Rheological techniques, small-angle neutron scattering (SANS), and transmission electron microscopy (TEM) are used to characterize the thermogels. We attribute the onset of thermogelling to depletion flocculation of the laponite particles into a network by spherical micelles of PF127.

### 1. Introduction

Thermogelling refers to the transformation of a fluid from a low-viscosity liquid (sol) to an elastic solid (gel) upon heating above a critical temperature.<sup>1–4</sup> This behavior is unusual because most types of structured complex fluids tend to decrease in viscosity with increasing temperature. Thermogelling has been observed in several systems, including those based on polysaccharides,<sup>5,6</sup> hybrid supramolecules,<sup>7</sup> and block copolymers.<sup>8,9</sup> Applications have been proposed for thermogelling fluids in areas such as drug delivery and tissue engineering,<sup>1–4</sup> heat-baked paints and coatings,<sup>10</sup> flow control in microfluidic devices,<sup>11</sup> matrices for capillary electrophoresis,<sup>12</sup> and fire fighting. For example, in the case of drug delivery and other biomedical applications,<sup>1–4</sup> the utility of thermogelling aqueous fluids is that they can be injected as thin solutions at room temperature but rapidly form gels inside the body at 37 °C; the resulting gelation thereby serves to localize an embedded drug at the site of injection. In fire fighting, a product termed Thermo-Gel has been recently commercialized; it is water containing a thermogelling agent and is claimed to be more effective than water at putting out fires.

A popular class of thermogelling aqueous systems are those based on the commercially available triblock copolymer

Pluronic F127 (PF127), also called Poloxamer 407.<sup>9,13</sup> The material is of the form PEO-PPO-PEO, where PEO refers to poly(ethylene oxide) and PPO refers to poly(propylene oxide). The approximate formula of PF127 is (EO)<sub>99</sub>(PO)<sub>65</sub>(EO)<sub>99</sub>. PF127 is used as a stabilizing agent for many colloidal dispersions in water.<sup>14–16</sup> This is because the hydrophobic PPO block tends to adsorb on particle surfaces while the hydrophilic PEO blocks extend into solution and provide steric stabilization to the particles.<sup>15</sup> The amphiphilic character of PF127 also allows it to form spherical micelles in water. With increasing concentration and temperature, the micellization tendency of PF127 is enhanced and in turn the volume fraction of spherical PF127 micelles rapidly increases.<sup>17–20</sup> Solutions of ≥15 wt % PF127 display thermogelling.<sup>17,21</sup> The onset of thermogelling occurs around 40 °C for 15% PF127 and corresponds to the spherical PF127 micelles filling up the volume in a jammed array ("micellar gel"). As the PF127 concentration is increased, thermogelling sets in at lower temperatures. The onset of thermogelling at a given PF127 concentration can be tweaked by the addition of salts,<sup>17,22</sup> sugars,<sup>22</sup> or hydrophobic drugs.<sup>23</sup> However, it is generally accepted in the literature that thermogelling requires concentrated (>15 wt %) solutions of PF127. Most studies and applications of PF127 have therefore focused on concentrated systems.

In this article, we show that thermogelling can occur at much lower concentrations of PF127 (as low as 1.2 wt %) provided nanoparticles of laponite are also present in the fluid at low concentrations. Our observations of thermogelling in

- \*Corresponding author. E-mail: sraghava@umd.edu.
- (1) Bromberg, L. E.; Ron, E. S. *Adv. Drug Delivery Rev.* **1998**, *31*, 197.  
(2) Jeong, B.; Kim, S. W.; Bae, Y. H. *Adv. Drug Delivery Rev.* **2002**, *54*, 37.  
(3) Ruel-Gariépy, E.; Leroux, J. C. *Eur. J. Pharm. Biopharm.* **2004**, *58*, 409.  
(4) Klouda, L.; Mikos, A. G. *Eur. J. Pharm. Biopharm.* **2008**, *68*, 34.  
(5) Kobayashi, K.; Huang, C. I.; Lodge, T. P. *Macromolecules* **1999**, *32*, 7070.  
(6) Chemine, A.; Chaput, C.; Wang, D.; Combes, C.; Buschmann, M. D.; Hoemann, C. D.; Leroux, J. C.; Atkinson, B. L.; Binette, F.; Selmani, A. *Biomaterials* **2000**, *21*, 2155.  
(7) Kidowaki, M.; Zhao, C. M.; Kataoka, T.; Ito, K. *Chem. Commun.* **2006**, *4102*.  
(8) Jeong, B.; Kibbey, M. R.; Birnbaum, J. C.; Won, Y. Y.; Gutowska, A. *Macromolecules* **2000**, *33*, 8317.  
(9) Escobar-Chavez, J. J.; Lopez-Cervantes, M.; Naik, A.; Kalia, Y. N.; Quintanar-Guerrero, D.; Ganem-Quintanar, A. *J. Pharm. Pharm. Sci.* **2006**, *9*, 339.  
(10) Lambourne, R.; Strivens, T. A. *Paint and Surface Coatings: Theory and Practice*, 2nd ed.; William Andrew Publishing: Norwich, NY, 1999.  
(11) Stoeber, B.; Hu, C. M. J.; Liepmann, D.; Muller, S. *J. Phys. Fluids* **2006**, *18*.  
(12) Wu, C. H.; Liu, T. B.; Chu, B. J.; Schneider, D. K.; Graziano, V. *Macromolecules* **1997**, *30*, 4574.  
(13) Alexandridis, P.; Hatton, T. A. *Colloids Surf. A* **1995**, *96*, 1.  
(14) Lin, Y. N.; Alexandridis, P. *J. Phys. Chem. B* **2002**, *106*, 10834.  
(15) Nelson, A.; Cosgrove, T. *Langmuir* **2005**, *21*, 9176.  
(16) Sun, K. S.; Kumar, R.; Falvey, D. E.; Raghavan, S. R. *J. Am. Chem. Soc.* **2009**, *131*, 7135.  
(17) Malmsten, M.; Lindman, B. *Macromolecules* **1992**, *25*, 5440.  
(18) Wanka, G.; Hoffmann, H.; Ulbricht, W. *Macromolecules* **1994**, *27*, 4145.  
(19) Mortensen, K.; Talmon, Y. *Macromolecules* **1995**, *28*, 8829.  
(20) Lam, Y. M.; Grigorieff, N.; Goldbeck-Wood, G. *Phys. Chem. Chem. Phys.* **1999**, *1*, 3331.  
(21) Prudhomme, R. K.; Wu, G. W.; Schneider, D. K. *Langmuir* **1996**, *12*, 4651.  
(22) Jiang, J.; Li, C.; Lombardi, J.; Colby, R. H.; Rigas, B.; Rafailovich, M. H.; Sokolov, J. C. *Polymer* **2008**, *49*, 3561.  
(23) Sharma, P. K.; Bhatia, S. R. *Int. J. Pharm.* **2004**, *278*, 361.

laponite/PF127 arose as an offshoot of recent work<sup>16,24</sup> with such mixtures in the context of light-responsive fluids. A brief mention of thermogelling in laponite/PF127 dispersions was made in our earlier paper,<sup>16</sup> and similar results have also been reported recently by a different group.<sup>25</sup> Laponite is a synthetic clay that exists as nanoscale disks, 25 nm in diameter and 0.9 nm in thickness.<sup>26</sup> PF127 and other Pluronic triblocks<sup>15,27–29</sup> are known to provide steric stabilization to laponite particles, and we use sufficient PF127 to saturate the particles completely (which corresponds to at least 0.3 g of PF127/g of laponite<sup>15</sup>). Our laponite/PF127 mixtures are thus stable, low-viscosity sols at room temperature. Also, at the concentrations of PF127 employed here (up to ~8 wt %), aqueous solutions of PF127 alone do not thermogel or show any appreciable increase in viscosity with temperature. Nevertheless, stable aqueous mixtures of a few wt % each of laponite and PF127 undergo thermogelling (i.e., a sol-to-gel transition upon heating). This phenomenon is robust and reversible (i.e., the gels revert to sols upon cooling), and the samples can be repeatedly cycled between sol and gel states by varying the temperature.

The challenge in this study is to decipher the mechanism for thermogelling in laponite/PF127 mixtures. Toward this end, we have characterized the microstructure of our samples using small-angle neutron scattering (SANS) and transmission electron microscopy (TEM). The evidence suggests that thermogelation is not due to the close packing of PF127 micelles but instead is due to the clustering of laponite nanoparticles into a fractal network. Furthermore, we suggest that the most likely mechanism for explaining laponite clustering at high (but not low) temperature involves depletion flocculation induced by free (nonadsorbing) PF127 micelles.

## 2. Experimental Section

**Materials.** Laponite RD was obtained from Southern Clay Products. Pluronic F127 (PF127) was reagent grade and was purchased from Sigma-Aldrich. Its overall molecular weight was 12 kDa. Deionized water from a Millipore water-purification system was used in preparing samples. For the SANS studies, the water was replaced with D<sub>2</sub>O (99.95% deuterated, from Cambridge Isotopes).

**Sample Preparation.** Dispersions of laponite particles were prepared by adding the particles to deionized water, followed by vortex mixing for 5 min. A Branson 1510 sonicator was then used for 1 h at 40 kHz to disperse the particles fully. Weighed quantities of PF127 were then added to the laponite dispersions, and the mixture was stirred continuously overnight to ensure that the final sample was completely homogeneous. The pH of these dispersions was found to be about 10.

**Rheological Studies.** Steady and dynamic rheological experiments were performed on an AR2000 stress-controlled rheometer (TA Instruments, Newark, DE). Samples were run on a cone-and-plate geometry (40 mm diameter, 4° cone angle) or a Couette geometry (rotor of radius 14 mm and height 42 mm, cup of radius 15 mm). For experiments at different temperatures, experiments were performed 20 min after equilibrating the loaded sample to the desired temperature. Dynamic frequency spectra were

(24) Sun, K. S. *Self-Assembled Photoresponsive and Thermoresponsive Nanostructures*. Ph.D. Dissertation, University of Maryland, 2009.

(25) Wu, C. J.; Schmidt, G. *Macromol. Rapid Commun.* **2009**, *30*, 1492.

(26) Cummins, H. Z. *J. Non-Cryst. Solids* **2007**, *353*, 3891.

(27) De Lisi, R.; Gradzielski, M.; Lazzara, G.; Milioto, S.; Muratore, N.; Prevost, S. *J. Phys. Chem. B* **2008**, *112*, 9328.

(28) Boucenna, I.; Royon, L.; Colinart, P. *J. Therm. Anal. Calorim.* **2009**, *98*, 119.

(29) Lazzara, G.; Milioto, S.; Gradzielski, M.; Prevost, S. *J. Phys. Chem. C* **2009**, *113*, 12213.

obtained in the linear viscoelastic regime of each sample, as determined by dynamic strain-sweep experiments.

**Small-Angle Neutron Scattering (SANS).** SANS measurements were made on the NG-7 (30 m) beamline at NIST in Gaithersburg, MD. Neutrons with a wavelength of 6 Å were selected. Three sample-detector distances of 1, 4, and 13 m were used to probe wave vectors from 0.004 to 0.4 Å<sup>-1</sup>. Samples were studied in 2 mm quartz cells at 25 and 80 °C. Scattering spectra were corrected and placed on an absolute scale using calibration standards provided by NIST.

**Transmission Electron Microscopy (TEM).** TEM was conducted on a Jeol JEM 2100 microscope at 80 KeV. The staining agent, uranyl acetate (UA) (from Sigma-Aldrich), was dissolved in water to form a 1% stock solution. One microliter of the laponite/PF127 sample was applied on two carbon/Formvar-coated copper grids, which were then dried separately at room temperature and at 80 °C, respectively. The dried TEM grids were then stained with a drop of the 1% UA solution and air-dried before imaging.

## 3. Results

**Thermogelling: Rheological Studies.** First we describe typical observations of the thermogelling phenomenon, followed by rheological studies. As a typical sample, consider a mixture of 3 wt % laponite and 3.6 wt % PF127 in deionized water, the photographs of which are shown in Figure 1. At room temperature, the dispersion is a low-viscosity sol that flows freely in the vial (Figure 1a). It is known that PF127 imparts steric stabilization to laponite particles, ensuring that the particles do not flocculate or aggregate.<sup>15</sup> Indeed, such laponite/PF127 sols remain stable and unchanged even months after preparation. Next, in Figure 1b, the same sample is photographed while being held in a water bath at 70 °C. The sample has been transformed into a gel at this higher temperature, as shown by its ability to hold its weight in the inverted vial. Note that the sample has a bluish hue but is homogeneous. The stirrer bar can be clearly seen to be trapped in the gel. No evidence of liquid-crystalline behavior (e.g., optical birefringence) was observed in the gel state.

We conducted rheological studies to quantify the temperature-induced changes in the rheology of the above sample. Figure 1a shows its dynamic rheology (elastic modulus  $G'$  and viscous modulus  $G''$  as functions of frequency  $\omega$ ) at 25 and 70 °C. At 25 °C, the sample shows a liquid-like response, as expected from its photograph. That is, it has a  $G''$  that is much greater than  $G'$  and both moduli are strong functions of frequency. In contrast, the response at 70 °C is solid-like (Figure 1b) i.e.,  $G' \gg G''$ , with both moduli independent of frequency. The latter response is typical of a permanent gel and is consistent with the photograph of the sample at this temperature. The frequency-independent value of  $G'$  is the gel modulus  $G_0$ , and it is approximately 200 Pa. Thus, dynamic rheology confirms the thermogelling transition in this sample.

Figure 2 shows steady-shear rheological data (viscosity vs shear stress) on the sample over a range of temperatures between 25 and 70 °C. At 25 °C, the sample is a Newtonian liquid with a viscosity of 4 mPa s (i.e., about 4 times the viscosity of the solvent, water). At 50 and 55 °C, the sample remains Newtonian and has about the same viscosity. At around the 60 °C mark, the viscosity begins to show a modest increase (by a factor of ~20). Further heating to 65 °C causes a sharp change in the rheology as the sample transforms from a liquid to a gel or yield-stress fluid. The viscosity is essentially infinite at low stress but upon approaching a stress of ~10 Pa (arrow) the viscosity plummets by several orders of magnitude. Thus, 10 Pa is the approximate yield stress of the sample at 65 °C. A further increase in temperature to 70 °C causes

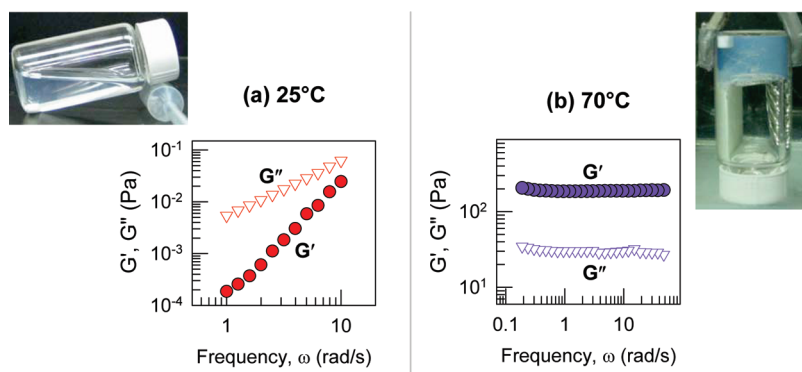


**Figure 1.** Dynamic rheology of a 3% laponite + 3.6% PF127 sample at (a) 25 °C and (b) 70 °C. At 25 °C, the sample shows a viscous response, and the photograph confirms that it is a freely flowing liquid. At 70 °C, the sample response is elastic and characteristic of a gel. The photograph shows the sample holding its weight in the inverted vial.

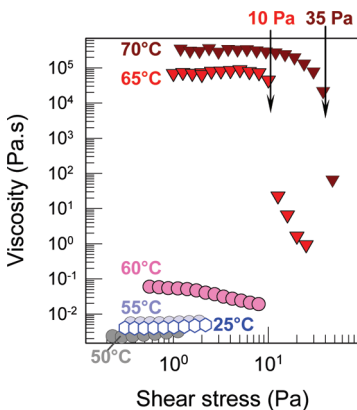


**Figure 2.** Steady-shear rheology of a 3% laponite + 3.6% PF127 sample at different temperatures. Around 65 °C, the sample abruptly transforms from a low-viscosity Newtonian fluid to a gel-like sample having a yield stress. The approximate values of the yield stress at 65 and 70 °C are marked by arrows.

an increase in the yield stress to about 35 Pa. Together, the data show that thermogelling is a drastic change in the sample rheology over a relatively narrow range of temperatures.

We have studied thermogelling over a range of laponite (0–wt %) and PF127 (0–8 wt %) concentrations. Figure 3 represents a state diagram over these ranges of concentration. Samples in the left corner of the diagram (dotted region, corresponding to <0.3 g of PF127/g of laponite) are not considered in our study because the particles in these dispersions are not completely stabilized;<sup>15</sup> thus, the samples are initially sols but age into viscous liquids. All other samples were sols at room temperature and remained so indefinitely (no aging effects). Among these samples, thermogelling occurs over the sample concentrations shaded in blue. Note that thermogelling requires critical concentrations of laponite and PF127 to be exceeded, and this point is further illustrated in Figures 4 and 5. Another point to be emphasized is that, given sufficient time, all of the samples in the thermogelling region revert to sols upon cooling (i.e., the phenomenon is a *reversible* rheological transition). The reversion to the sol state is instantaneous for some samples and takes several hours for others (the latter is typically the case at higher laponite and PF127 concentrations).

Figure 4 presents rheological data regarding the effect of laponite concentration on thermogelling. For these studies, the PF127 content was fixed at 1.7% and the laponite concentration was varied. All samples were thin Newtonian liquids at low

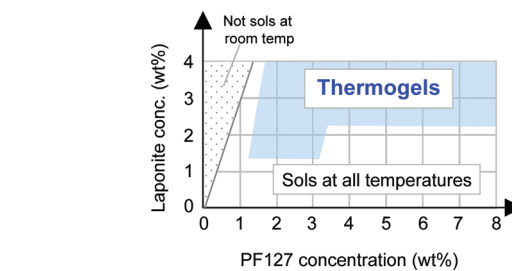


**Figure 3.** State diagram showing the concentration range of laponite/PF127 aqueous solutions over which reversible thermogelling is observed. (See the text for details.)

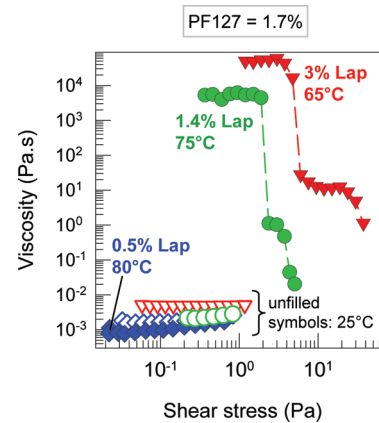


**Figure 4.** Effect of laponite concentration on thermogelling. Steady-shear data at 25 °C and high temperatures are shown for samples containing 1.7% PF127 and varying amounts of laponite. Data at 25 °C are shown with unfilled symbols, and those at high temperatures are shown with filled symbols. Thermogelling occurs only for laponite concentrations above a minimum value.

temperatures. At low laponite concentration (e.g., 0.5%), no temperature-induced viscosity increase is seen; in fact, the viscosity at 80 °C is slightly lower than that at 25 °C. At a higher laponite concentration of 1.4%, the system gels at 75 °C with a yield stress of 2 Pa. A further increase in laponite concentration to 3% reduces the gelling temperature to 65 °C whereas the yield stress increases to 4 Pa. Thus, a minimum amount of laponite needs to be present for thermogelling. This is consistent with Figure 3 as well – note that PF127 on its own does not undergo thermogelling over the range of 0 to 8 wt %.<sup>17,19,21</sup> To reiterate, thermogelling of PF127 alone occurs only at much higher

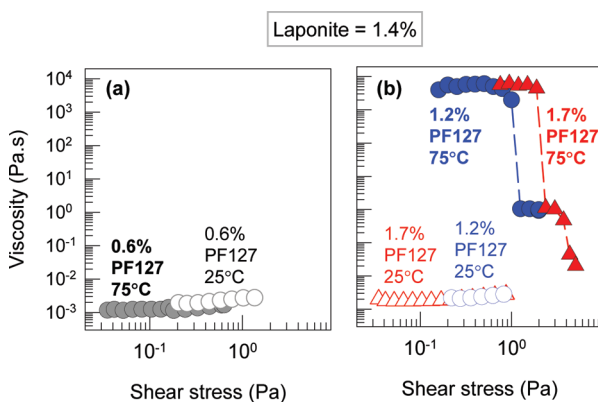


**Figure 5.** Effect of PF127 concentration on thermogelling. Steady-shear data are shown for samples containing 1.4% laponite and varying amounts of PF127 at 25 and 75 °C. Data at 25 °C are shown with unfilled symbols, and those at high temperatures are shown with filled symbols. Thermogelling does not occur at low concentrations such as 0.6% PF127, as shown in a. It does occur for 1.2 and 1.7% PF127, as shown in b.

concentrations (~15 wt %) and is attributed to the formation of a close-packed array of PF127 micelles.<sup>17,21</sup> The phenomenon seen here is of a different nature. It is not simply due to PF127 but rather requires both PF127 and laponite to be present.

The effect of PF127 concentration at constant laponite concentration (1.4%) is displayed in Figure 5. No thermogelling is seen for a low concentration of PF127 such as 0.6%; the viscosity of this sample is again slightly lower at 75 °C than at 25 °C (Figure 5a). Note that 0.6% PF127 is sufficient to stabilize 1.4% laponite and the sample remains a stable sol with no aging effects. When PF127 is increased to 1.2 or 1.7%, thermogelling occurs (Figure 5b). Both samples gel at 75 °C, with the yield stress being slightly higher for the 1.7% sample. Thus, PF127 also needs to be present above a minimum level for thermogelling to occur. Intriguingly, if PF127 is increased to around 4% or higher, the sample reverts to a sol; this can be seen in Figure 3 where a horizontal line (constant laponite concentration) enters the thermogel region and then exits. This unusual sol–gel–sol behavior was not observed at higher laponite concentrations, however.

**Thermogelling: Microstructural Studies.** To gain insight into the thermogelling mechanism, we attempted to characterize the structure of the samples using SANS and TEM. Samples for SANS were made in D<sub>2</sub>O to attain the required scattering contrast. For an accurate comparison with our aqueous samples, we accounted for the density of D<sub>2</sub>O; therefore, the concentrations in D<sub>2</sub>O correspond to the identical w/v % of those in water. Figure 6 shows SANS spectra ( $I$  vs  $q$ ) for two samples at 25 and 80 °C. The first contains 0.5% laponite and 0.6% PF127; this sample has low concentrations of laponite and PF127 and does not undergo thermogelling. The second sample contains 1.4% laponite and 1.7% PF127 and does thermogel around 75 °C. Both samples exhibit similar features in their SANS spectra. At 25 °C, the intensity  $I$  shows a plateau at low  $q$ , which suggests that the laponite particles are well-dispersed and stable. At 80 °C, a significant rise in  $I$  at low  $q$  is seen for both samples. The only difference is that  $I$  seems to be tapering to a plateau for the non-thermogelling sample, whereas  $I$  for the thermogelling sample continues to increase (diverges).

The SANS data allow us to tackle an initial question about thermogelling: is this due to the clustering of laponite particles or the close-packing of PF127 micelles? In this context, it is worth comparing the spectra in Figure 6 to those from PF127 alone.

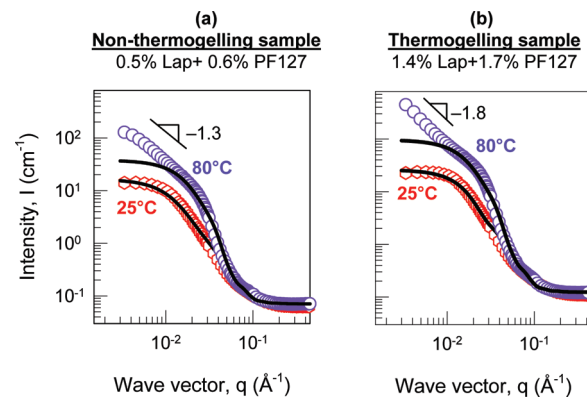


**Figure 6.** SANS scattering spectra (intensity  $I$  vs wave vector  $q$ ) at 25 and 80 °C for samples containing (a) 0.5% laponite + 0.6% PF127 and (b) 1.4% laponite + 1.7% PF127. The data are fit to models (see the text for details), and the model fits are shown as solid lines through the data.

SANS data on PF127 solutions have been reported by several authors,<sup>19,21,23</sup> and the data are typical of spherical micelles at low PF127 (1 to 2%) with a plateau in  $I$  at low  $q$ . At higher PF127 (>4%), an interaction peak is seen at intermediate  $q$  that is reflective of repulsive excluded-volume interactions between the micelles.<sup>19,21</sup> An increase in  $I$  at low  $q$ , which signifies the growth of large structures such as fractal networks,<sup>30</sup> is *not* observed for PF127 over the range of temperature. On the other hand, in our earlier study on a photogelling laponite/PF127 system,<sup>16</sup> we did find a diverging  $I$  at low  $q$  in instances where laponite formed gels. (In that case, gelation was triggered by light, not heat, and the network was of the “house-of-cards” type.) Thus, in light of earlier studies, it is reasonable to assume that the high-temperature SANS data in Figure 6 reflect the clustering of laponite particles.

The above SANS data are quite complex because the scattering curves have contributions from both the laponite particles and the PF127 unimers/micelles. In an attempt to model the data, we make the following assumptions. We assume that the structures present in the samples will be (a) laponite disks covered with adsorbed PF127 and (b) spherical PF127 micelles in the bulk. In the sol state at 25 °C, the disks will be distinct and unaggregated. Thus, we can model the system on the basis of the form factors for core–shell disks (laponite core and PF127 shell) and core–shell spheres (micelles or monomers of PF127, both with PPO cores and PEO shells).<sup>15,16,31</sup> The equations and fitting parameters are provided as part of the Supporting Information. For the modeling, we fix the dimensions of the laponite core to have a diameter of 25 nm and a thickness of 0.9 nm. From model fitting, we find that the PF127 shell is 1.6 nm thick over both the particle face and edge. The PF127 spheres are found to have a PPO core with a 1.6 nm diameter and a PEO shell with a 0.4 nm thickness; these small sizes are mostly indicative of unmicellized PF127 monomers. With these parameters, we are able to fit the data for both samples at 25 °C, with the only difference being the particle and monomer volume fractions.

For the data at 80 °C, we use the same form-factor models as above. We find that the shell of PF127 on the laponite particles is thicker (5.4 nm over the face, 2.8 nm over the edge). This means that the clustering particles are not bare laponite but laponite covered with a thick stabilizing layer of polymer. The PF127 spheres are also larger, with a core diameter of 7.6 nm and a shell thickness of 2.2 nm; these larger sizes are indicative of PF127

(30) Teixeira, J. *J. Appl. Crystallogr.* **1988**, *21*, 781.

(31) Pedersen, J. S. *Adv. Colloid Interface Sci.* **1997**, *70*, 171.

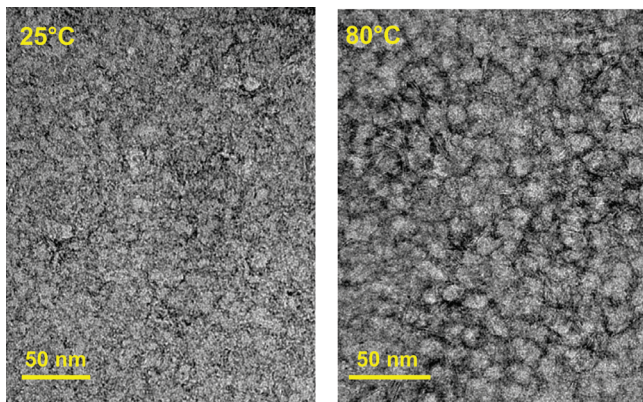


**Figure 7.** TEM images corresponding to a 0.5% laponite + 0.6% PF127 sample at 25 °C (left) and 80 °C (right). The images are stained with uranyl acetate. The image on the right shows a large number of PF127 micelles.

micelles. As mentioned earlier, it is known that PF127 monomers increasingly assemble into micelles as the temperature is increased.<sup>17–20</sup> The overall micelle size of 12.0 nm from above is close to that reported in other studies.<sup>19,20</sup> It is clear that our form factor model does not account for the increased scattering at low  $q$ , for which a structure factor model, such as for fractal clusters,<sup>30</sup> is necessary. However, the fractal structure factor cannot be combined in a straightforward manner with form factor models, especially when the particles are not spherical but disklike. Note that the thermogelling sample at 80 °C (Figure 6b) shows a power-law scaling at low  $q$  with a slope of  $-1.8$ . The nonthermogelling sample at 80 °C has a lower scaling exponent and its scattered intensity tapers out into a plateau at low  $q$ . These differences imply more clustering and/or larger clusters in the thermogelling sample. Thus, altogether, the modeling suggests clustered particles in the thermogelled sample and also indicates larger PF127 micelles and thicker adsorbed layers of PF127 at the higher temperature. Additional refinements to the SANS modeling are beyond the scope of the present work. Future modeling would be facilitated if SANS data could be obtained under conditions where either the laponite or the PF127 was contrast-matched with the solvent.

Further evidence for an abundance of PF127 micelles at high temperatures was obtained from TEM analysis. These experiments had to be conducted with a dilute mixture of laponite and PF127 to allow structural details to be resolved. We therefore worked with a sample of 0.5% laponite + 0.6% PF127, and we used uranyl acetate as a negative stain. As described in the Experimental Section, our procedure involved placing a drop of the sample on a TEM grid and drying at either 25 or 80 °C, followed by staining. (During the drying process, the concentrations in solution are expected to increase and possibly fall within the thermogelling range.<sup>20</sup>) The image in Figure 7 for the sample at 80 °C appears to reveal numerous PF127 micelles of  $\sim 10$  nm in diameter, which is consistent with the SANS results. In comparison, the image corresponding to the sample at 25 °C is featureless. It is not possible to resolve individual laponite particles in any of the images, possibly because the disks are less than a nanometer thick. The TEM results confirm that relatively large PF127 micelles are present in the sample at high temperature and that these micelles occupy a considerable volume fraction.

#### 4. Discussion

As mentioned in the Introduction, numerous additives have been studied for their effects on PF127 thermogelling.<sup>17,22,23,28</sup> Such studies have typically been carried out with  $\geq 15$  wt % PF127

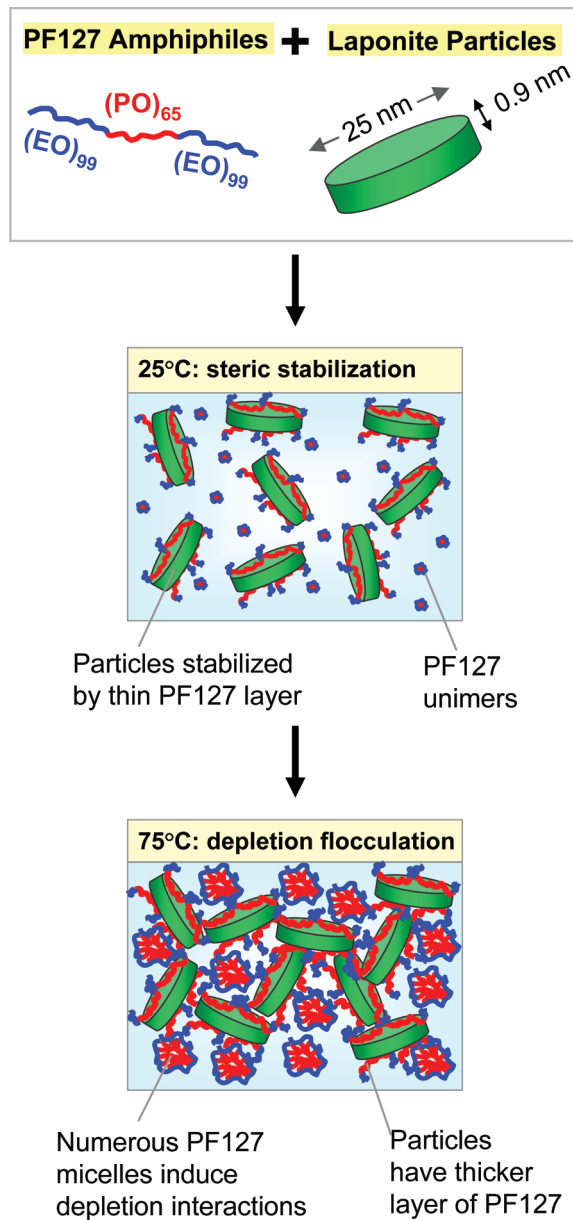


**Figure 8.** Mechanism for thermogelling in laponite/PF127 mixtures. The PF127 triblock copolymer is shown with its PPO segment in red and its PEO segments in blue. At low temperatures, the PF127 chains stabilize the particles: the red PPO segments are shown to be adsorbed on the particle surface, and the blue PEO segments extend into solution. Excess PF127 also exists in solution in the form of unimers or small micelles. At high temperatures, the solution undergoes thermogelling. This is shown to be due to the clustering of laponite particles into a volume-filling network. The driving force is depletion interactions induced by PF127 micelles. Each micelle is shown with a PPO core and a PEO shell, and the micelles occupy a considerable volume fraction. The particles actually have a thicker shell of PF127 than at low temperatures—so there is no direct interaction between the particle surface and the micelles. Depletion is strictly an osmotic effect caused by the free (nonadsorbing) micelles.

(i.e., above its gelation threshold). The influence of the above additives is then mainly to alter the close-packing of micelles within a PF127 thermogel. For example, many salts lower the thermogelation temperature, and the reason for this is that salts increase the micelle size at a given temperature, allowing the micelles to reach close-packing sooner.<sup>17,22</sup> Thermogelling in laponite/PF127, in contrast, cannot be rationalized on the basis

of the close-packing of PF127 micelles. At the PF127 concentrations studied here (as low as 1.2 wt %), the micelle volume fraction is far short of close packing. Also, the growth of PF127 micelles (e.g., from spheres to cylinders) is not a likely explanation because cylindrical micelles at low concentrations cannot form gels with yield stresses. On the other hand, it is indeed possible for laponite particles to form volume-filling networks at ~1 wt % in water.<sup>16,26</sup> With this in mind, we proceed to discuss possible mechanisms for thermogelling in laponite/PF127 mixtures. Below we present three possibilities and critically examine the evidence for each one.

**Mechanism 1. Flocculation of Bare Laponite Particles.** The first and simplest possibility is that the laponite particles lose their stabilizing shell of PF127 upon heating, which leads to direct contact between bare particles and in turn their flocculation. As mentioned earlier, this mechanism is not consistent with our results from SANS modeling, which show that the PF127 layer on each particle becomes *thicker*, not thinner, with heating. This finding is consistent with the idea that the adsorption of PF127 will be promoted at high temperatures because, under those conditions the PPO segment tends to become more hydrophobic.<sup>17–20</sup> Other experimental results are also not consistent with the above mechanism. For example, if thermogelling was due to direct contact between bare laponite particles, then the lower the PF127 concentration, the higher should be its propensity to occur. Instead, Figure 4 indicates that thermogelling does not occur if the PF127 concentration is too low. In sum, the data do not support this first mechanism.

**Mechanism 2. Stickiness of PF127 Layers on Laponite.** A second possibility is that the laponite disks remain covered with a layer of PF127 over the entire range of temperatures but that these surface layers become “sticky” at high temperatures. Such stickiness or attractive interactions between adjacent particles could be visualized to occur (a) by the direct sticking of PEO segments extending from the surfaces of two adjacent particles or (b) by individual PF127 micelles (or possibly chains of such micelles) bridging adjacent particles. This mechanism is somewhat akin to bridging flocculation of particles by polymers.<sup>32</sup> However, to our knowledge, there is no evidence that PF127 chains or micelles become sticky (aggregate) over the temperature range studied here. Indeed, large volume fractions of PF127 micelles are known to coexist in a stable cubic phase for PF127 > 25 wt %.<sup>21</sup> Also, bridging flocculation is most likely to occur when the particles are incompletely covered with stabilizing polymer<sup>32</sup> (i.e., at low PF127 concentrations relative to laponite concentrations). However, once again, Figures 3 and 4 show that amounts of PF127 that are too low amounts of PF127 are detrimental to thermogelling, which contradicts this mechanism.

**Mechanism 3. Depletion Flocculation by Free PF127 Micelles.** A third possibility is that thermogelling is due to the depletion flocculation of laponite particles induced by free PF127 micelles. Depletion flocculation is an osmotic effect originally proposed to describe the flocculation of colloidal particles by nonadsorbing polymers.<sup>32,33</sup> It is now known that depletion interactions can be caused by other species as well, including surfactant micelles.<sup>33,34</sup> For example, when a surfactant is added to particles or emulsion droplets, it initially adsorbs on the particles and stabilizes them. As further surfactant is added, however, the excess unadsorbed surfactant assembles into micelles in solution, which can then cause the particles or droplets

to flocculate via a depletion mechanism.<sup>33,34</sup> We believe that a similar effect occurs in laponite/PF127 mixtures.

Consider laponite particles stabilized by a layer of PF127. In a thermogelling sample at ~75 °C, the particles will coexist with a relatively high volume fraction of spherical PF127 micelles (Figure 8). The particle size, including the PF127 shell, is ~31 nm in diameter and 12 nm in thickness, while the PF127 micelles are about 12 nm in diameter. When the laponite particles approach each other by Brownian motion to a distance less than about 12 nm, the PF127 micelles will be depleted in the zone between the particles. The higher concentration of micelles in the bulk compared to that in the depletion zone will then force the particles together, causing flocculation,<sup>32,33</sup> and this is depicted in Figure 8. Being an osmotic effect, this mechanism does not presuppose any direct interaction between the micelles and the particles. The (attractive) depletion potential is enhanced by having more micelles of the same size, and the range of the interaction is set by the micelle size.<sup>32,33</sup>

How is the depletion mechanism consistent with our results? First, it can explain why the laponite particles flocculate at high and not at low temperatures. Depletion requires an abundance of PF127 micelles, which is the case only at high temperatures, as seen from our SANS and TEM data. Second, it explains why thermogelling does not occur at low PF127 (insufficient micelles to cause depletion) or low laponite concentrations (particles too far apart on average to experience the potential). Also, depletion interactions usually correspond to a weak potential well, implying the weak, reversible flocculation of the particles,<sup>32,33</sup> and this might be the key to ensuring the reversible nature of the thermogelling observed here. All in all, this mechanism fits a number of facts, although further studies will be needed to prove its correctness conclusively. In terms of predictions for future studies, any variable that increases the size or volume fraction of PF127 micelles should in turn lead to a reduction in thermogelation temperature. Another prediction would be that depletion flocculation via PF127 micelles at high temperatures should also occur for other types of particles, not just laponite.

## 5. Conclusions

We have demonstrated thermogelling in laponite/PF127 mixtures. At room temperature, PF127 adsorbs onto laponite particles and stabilizes them by steric repulsion. Upon heating, the PF127 layers on the particles become thicker and, more importantly, PF127 micelles in the bulk solution become significantly more abundant. At a distinct temperature, the free PF127 micelles induce the *depletion flocculation* of the laponite particles into a gel network. Thermogelling occurs only if there is sufficient PF127 (at least ~1.2 wt %) as well as sufficient laponite (at least ~1.4 wt %) in the sample. The phenomenon is reversible (i.e., the gels revert to liquids upon cooling). Thermogelling PF127/laponite mixtures could find application in a variety of areas including heat-based coatings and drug delivery. Because only low concentrations of the two components are required, the combination could prove to be a cost-effective thermogelling agent.

**Acknowledgment.** This work was partially funded by a CAREER award from NSF-CBET. We acknowledge NIST NCNR for enabling the SANS experiments performed as part of this work. Additionally, we acknowledge the Maryland Nano-Center for facilitating the TEM experiments reported here.

**Supporting Information Available:** Details of SANS modeling in Figure 6. This material is available free of charge via the Internet at <http://pubs.acs.org>.

(32) Hunter, R. J. *Foundations of Colloid Science*; Oxford University Press: Oxford, U.K., 2001.

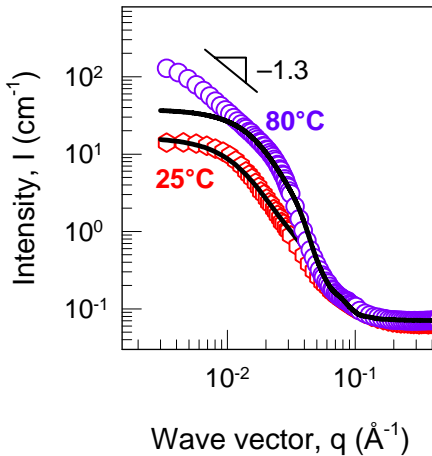
(33) Tuinier, R.; Rieger, J.; de Kruif, C. G. *Adv. Colloid Interface Sci.* **2003**, *103*, 1.

(34) Wang, H.; Zhou, W.; Ho, D. L.; Winey, K. I.; Fischer, J. E.; Glinka, C. J.; Hobbie, E. K. *Nano Lett.* **2004**, *4*, 1789.

## Supporting Information for

Thermogelling Aqueous Fluids Containing Low Concentrations of Pluronic F127 and Laponite Nanoparticles

Kunshan Sun and Srinivasa R. Raghavan\*



Each curve modeled as:

**Form Factor for Core-Shell Disks** = Laponite covered with PF127 =  $P_1(q)$  +

**Form Factor for Core-Shell Spheres** = PF127 micelles =  $P_2(q)$

(Structure Factor  $S(q) = 1$ , i.e., no interactions)

**Core-Shell Disks:** see schematic from Nelson and Cosgrove (Ref. 15)

Core of the disk = laponite (25 nm diameter, 0.9 nm radius)

Shell of the disk = PF127



Form factor for core-shell disks:

$$P_1(q) = \frac{1}{\langle V_p \rangle} \int_0^{\pi/2} \sin \theta d\theta \left\{ V_1 (\rho_1 - \rho_{\text{solv}}) \frac{\sin[q(H_p + 2\Delta H)(\cos \theta)/2]}{q(H_p + 2\Delta H)(\cos \theta)/2} \frac{2J_1[q(R_p + \Delta R)\sin \theta]}{q(R_p + \Delta R)\sin \theta} + V_p (\rho_p - \rho_1) \frac{\sin[qH_p(\cos \theta)/2]}{qH_p(\cos \theta)/2} \frac{2J_1[qR_p \sin \theta]}{qR_p \sin \theta} \right\}^2$$

$$\text{where } J_1(x) = \frac{\sin x - x \cos x}{x^2}$$

### Parameters (Core):

$\langle V_p \rangle$  = average volume of core

$V_p$  = volume of core

$R_p$  = radius of core = 25 nm

$H_p$  = thickness of core = 0.9 nm

$\rho_p$  = scattering length density of the core

### Parameters (Shell):

$\Delta R$  = shell thickness on the edge

$\Delta H$  = shell thickness on the face

$\rho_1$  = scattering length density of the shell

### Parameters (Other):

$V_1$  = total volume of particle core and shell

$\rho_{\text{solv}}$  = scattering length density of the solvent

**Core-Shell Spheres:** see Pedersen (Ref. 31)

$$P_2(q) = \frac{1}{\langle V_m \rangle} \int_0^{r=\infty} f(r) F^2(qr) dr \quad \text{where } F(qr) = p^3 (\rho_c - \rho_s) V_m \frac{3J_1(qpr)}{qpr} + (\rho_s - \rho_{solv}) V_m \frac{3J_1(qr)}{qr}$$

**Parameters:**

$\langle V_m \rangle$  = average volume of sphere  
 $V_m$  = volume of the sphere  
 $r$  = overall radius (core+shell)  
 $pr$  = radius of core  
 $\rho_c$  = scattering length density of the core  
 $\rho_s$  = scattering length density of the shell  
 $\rho_{solv}$  = scattering length density of the solvent  
 $f(r)$  = Schulz distribution for the polydispersity of the radius

**SANS Modeling: Key Parameters with Error Bars**

<b>Key Parameters</b>	0.5% lap + 0.6% PF127		1.4% lap + 1.7% PF127	
	25°C	80°C	25°C	80°C
Edge shell thickness (nm)	1.6 $\pm$ 0.013	2.8 $\pm$ 0.027	1.6 $\pm$ 0.007	2.8 $\pm$ 0.019
Face shell thickness (nm)	1.6 $\pm$ 0.001	5.4 $\pm$ 0.006	1.6 $\pm$ 0.001	5.4 $\pm$ 0.004
Micelle core diameter (nm)	1.6 $\pm$ 0.005	7.6 $\pm$ 0.004	1.6 $\pm$ 0.003	7.6 $\pm$ 0.004
Micelle shell thickness (nm)	0.4 $\pm$ 0.003	2.2 $\pm$ 0.003	0.4 $\pm$ 0.002	2.2 $\pm$ 0.002